Cell, Vol. 121, 515–527, May 20, 2005, Copyright ©2005 by Elsevier Inc. DOI 10.1016/j.cell.2005.03.035

Assembly of the SIR Complex and Its Regulation by *O*-Acetyl-ADP-Ribose, a Product of NAD-Dependent Histone Deacetylation

Gunn-Guang Liou,[1] Jason C. Tanny,[1,3] Ryan G. Kruger,[2] Thomas Walz,[1] and Danesh Moazed[1,*]
[1]Department of Cell Biology
[2]Department of Biochemistry and Molecular Pharmacology
Harvard Medical School
Boston, Massachusetts 02115

Summary

Assembly of silent chromatin domains in budding yeast involves the deacetylation of histone tails by Sir2 and the association of the Sir3 and Sir4 proteins with hypoacetylated histone tails. Sir2 couples deacetylation to NAD hydrolysis and the synthesis of a metabolite, *O*-acetyl-ADP-ribose (AAR), but the functional significance of NAD hydrolysis or AAR, if any, is unknown. Here we examine the association of the Sir2, Sir3, and Sir4 proteins with each other and histone tails. Our analysis reveals that deacetylation of histone H4-lysine 16 (K16), which is critical for silencing in vivo, is also critical for the binding of Sir3 and Sir4 to histone H4 peptides in vitro. Moreover, AAR itself promotes the association of multiple copies of Sir3 with Sir2/Sir4 and induces a dramatic structural rearrangement in the SIR complex. These results suggest that Sir2 activity modulates the assembly of the SIR complex through both histone deacetylation and AAR synthesis.

Introduction

Silent chromatin domains play a central role in the regulation of gene expression and maintenance of chromosome stability. In the budding yeast *Saccharomyces cerevisiae,* the *HM* mating-type loci and telomeres are packaged into silent chromatin (Gasser and Cockell, 2001; Rusche et al., 2003). In addition, silencing inhibits recombination within the ribosomal DNA (rDNA) locus, stabilizing this highly repetitive portion of the genome, which contributes to extension of replicative life span (Bryk et al., 1997; Gottlieb and Esposito, 1989; Guarente, 2000; Smith and Boeke, 1997). Silent chromatin in budding yeast is functionally analogous to heterochromatin, a widely conserved feature of eukaryotic chromosomes that is required for chromosome stability (Grewal and Moazed, 2003).

Research in a number of biological systems indicates fundamental similarities in the molecular mechanisms that assemble silent chromatin domains (Moazed, 2001). Silencing proteins are initially recruited to chromatin via sequence-specific interactions at silencing "initiation" regions. Then, sequence-nonspecific "spreading" occurs, whereby large chromosomal regions are coated with silencing proteins. Current models predict that two types of interactions underlie the "spreading" phenomenon: interactions among various silencing proteins themselves and interactions between one or more silencing proteins and the conserved amino termini of histones H3 and H4. Spreading is thought to be triggered by a histone-modifying activity in one of the silencing proteins, which, upon its initial binding to chromatin, modifies adjacent histone tails and increases their affinity for silencing proteins. Interactions between silencing proteins then bring in more of the modifying enzyme, allowing repeated cycles of histone modification and binding of silencing proteins.

In budding yeast, the Sir2, Sir3, and Sir4 proteins mediate silencing at *HM* loci and at telomeres, and their molecular functions are consistent with the above model (Aparicio et al., 1991; Klar et al., 1979; Rine and Herskowitz, 1987). Sir2 is a conserved NAD-dependent histone deacetylase that forms a highly stable complex with Sir4 in yeast extracts (Ghidelli et al., 2001; Imai et al., 2000; Landry et al., 2000; Moazed and Johnson, 1996; Moazed et al., 1997; Smith et al., 2000; Strahl-Bolsinger et al., 1997). Sir3 and, to a lesser extent, Sir4 both physically interact with the amino-terminal tails of histones H3 and H4, and these interactions are stimulated when the tails are hypoacetylated (Carmen et al., 2002; Hecht et al., 1995). Finally, Sir3 and Sir4 also interact, albeit less strongly than Sir2 and Sir4 (Hecht et al., 1996; Moazed et al., 1997; Moretti et al., 1994), and this interaction is essential for silencing and spreading of Sir proteins in vivo (Rudner et al., 2005). Thus, assembly of silent chromatin has been proposed to occur via initial binding of Sir2/Sir4, followed by histone deacetylation by Sir2, then Sir3 binding, and, finally, recruitment of additional Sir complexes to complete the cycle (Hoppe et al., 2002; Luo et al., 2002; Rusche et al., 2002).

In broad outline, this model is consistent with experimental data to date, but many mechanistic details still need to be clarified. First, the exact nature of the interactions between Sir proteins that mediate spreading is unknown. In addition to the strong interaction between Sir3 and Sir4, Sir3 also has been shown to self-associate (Enomoto et al., 2000; Moretti et al., 1994). The nature of this self-association, or its relevance for silent chromatin assembly, has yet to be established.

The interactions between Sir proteins and histones are also poorly defined. Previous experiments have shown that a C-terminal fragment of Sir3 has affinity for the H4 N-terminal tail and that the k_a for this interaction is increased when the tail is hypoacetylated at any of the invariant lysines in the H4 tail (Carmen et al., 2002). However, genetic experiments have demonstrated a specific role for hypoacetylation of H4-K16 in silencing and little if any role for K5, -8, and -12 (Johnson et al., 1990; Johnson et al., 1992). Also, the deacetylase activity of Sir2 is remarkably specific for H4-K16 in vitro (Imai et al., 2000; Tanny et al., 2004; Tanny and Moazed, 2001). The reasons for these discrepancies are unclear.

*Correspondence: danesh@hms.harvard.edu
[3]Present address: Laboratory of Chromatin Biology, Rockefeller University, New York, New York 10021.

Finally, the precise molecular function of Sir2 enzymatic activity has not been established. Sir2 is a member of a large family of enzymes that use NAD to catalyze a similar reaction that couples deacetylation to hydrolysis of NAD and the synthesis of a metabolite, *O*-acetyl-ADP-ribose (AAR) (Tanner et al., 2000; Tanny and Moazed, 2001). This unusual reaction involves the cleavage of the N-glycosidic bond between the ADP-ribose and nicotinamide moieties of NAD, resulting in the release of nicotinamide and the formation of 2′-AAR, which then undergoes *trans*-esterification to generate a mixture of 2′- and 3′-AAR stereoisomers (Jackson and Denu, 2002; Sauve et al., 2001). Mutations that disrupt the enzymatic activity of Sir2 abolish silencing in vivo (Imai et al., 2000; Tanny et al., 1999), although they allow some binding of Sir proteins to nucleation sites, suggesting that Sir2 activity contributes primarily to spreading of Sir proteins along chromatin. In principle, any one of several outcomes of Sir2 activity, including deacetylation, NAD hydrolysis, or AAR synthesis, could be crucial for silencing. Much attention has been focused on Sir2-mediated deacetylation because a large body of evidence provides a correlation between hypoacetylation of histone tails and silent chromatin (Braunstein et al., 1993; Grunstein, 1997a; Jenuwein and Allis, 2001). Mutational analysis of the conserved amino termini of histones H3 and H4 has identified several residues that are required for silencing (Johnson et al., 1990). In particular, amino acid substitutions that replace histone H4-K16 with amino acids that mimic the acetylated state disrupt silencing. However, deacetylation of H4-K16 cannot be the sole function of Sir2 since loss of Sir2 could not be suppressed by simultaneous removal of the major K16 acetyltransferase, Sas2 (Kimura et al., 2002; Suka et al., 2002). Interestingly, in this double mutant strain, some binding of Sir3 occurred close to silencing nucleation sites, but no spreading of Sir3 was observed. This suggests that Sir2 may promote spreading by some means other than histone deacetylation.

In this study we address these questions using an in vitro system composed of full-length Sir proteins purified from yeast and various peptides corresponding to the N-terminal tail of histone H4. Our results provide a detailed picture of the interactions between Sir proteins that contribute to silencing and yield new insight into specific recognition of histone tails by the SIR complex. Importantly, we provide evidence that AAR, the product of NAD-dependent deacetylation, is directly involved in regulating SIR-complex assembly.

Results

In order to obtain sufficient quantities of full-length Sir proteins for biochemical analysis, we developed a system based on protein overexpression in yeast cells. We constructed a strain that overexpresses HA-Sir2 and an amino-terminally TAP-tagged Sir4 protein from the inducible *GAL1* promoter (*GAL1-TAP-SIR4*, *GAL1-HA-SIR2*). TAP-tagged Sir3 was overproduced from a high copy 2 micron *GAL1* plasmid by itself (*GAL1-SIR3-TAP*). After induction on galactose, we obtained near-milligram amounts of a stoichiometric Sir2/Sir4 complex and Sir3 from each of the above strains, respectively (Figure 1A). In addition, we used baculovirus-produced Sir2 and bacterially produced Sir2, Sir3, and Sir4 fragments to confirm or extend previous observations on the interaction of Sir proteins with histones and each other.

An Extensive Network of Protein-Protein Interactions in the SIR Complex

Since the binding affinities for Sir-Sir interactions have not been measured using full-length proteins, we first used surface plasmon resonance (SPR) spectroscopy to investigate the interaction of immobilized Sir3 with the Sir2/Sir4 complex. Dissociation binding constants (K_D) were determined based on real-time measurements of *on* and *off* rates and showed that Sir2/Sir4 bound to Sir3 with a binding constant of $\sim 3 \times 10^{-11}$ M (Figures 1B and 1F). A binding site for Sir3 has previously been mapped to the extreme C-terminal coiled-coil region of Sir4 from amino acids 1198 to 1358 (Sir4-C1) (Chang et al., 2003). We found that Sir4-C1 bound to Sir3 with greatly reduced affinity ($K_D \sim 3 \times 10^{-8}$ M) (Figures 1D and 1F), suggesting that either Sir2 or other regions of Sir4 contribute to high-affinity binding of Sir2/Sir4 to Sir3. Consistent with this possibility, we found that Sir2 bound to Sir3 with a binding constant of $\sim 6 \times 10^{-8}$ M and that Sir3 bound to the C-terminal region of Sir4, corresponding to amino acids 745 to 1172 (Sir4-C2), with a binding constant of $\sim 1 \times 10^{-9}$ M. As a control, the substitution of isoleucine 1311 with asparagine in the C terminus of Sir4 (Sir4C1-I1311N), which has previously been shown to abolish its interaction with Sir3 (Chang et al., 2003; Rudner et al., 2005), also abolished the association of this Sir4 fragment with Sir3 in the SPR assays (Figures 1E and 1F). We were unable to examine the interaction of full-length Sir4 with Sir2 or Sir3 because in *sir2Δ* cells, Sir4-TAP was unstable and could not be purified (Figure S1). We verified the interaction of Sir3 with Sir2 and with Sir4-C2 using an independent pull-down assay and found that both Sir4-C2 and GST-Sir2 bound to calmodulin-Sepharose containing immobilized Sir3-CBP but not to empty calmodulin-Sepharose; moreover, Sir3 and Sir2-His_6 bound to GST-Sir2 but not to GST (data not shown). These results confirm previous two-hybrid and pull-down experiments (Hecht et al., 1996; Moazed et al., 1997; Moretti et al., 1994; Strahl-Bolsinger et al., 1997) and suggest that Sir2 and at least two different Sir4 regions contribute to the interaction of Sir2/Sir4 with Sir3.

Consistent with previous two-hybrid results (Enomoto et al., 2000; Moretti et al., 1994), we found that the Sir3 protein interacted with itself with a binding constant of $\sim 2 \times 10^{-9}$ M (Figure 1F). In addition, the binding of additional Sir3 to immobilized Sir3 on the SPR chip resulted in a 2-fold increase in the affinity for Sir2/Sir4 (Figures 1C and 1F), suggesting that self-association of Sir3 may result in an increase in its affinity for Sir4.

Association of the Sir3 and Sir4 Proteins with the N Terminus of Histone H4 Is Regulated by Acetylation of Lysine 16

Previous studies have established that (1) reticulocyte-lysate-synthesized and radioactively labeled Sir3 and

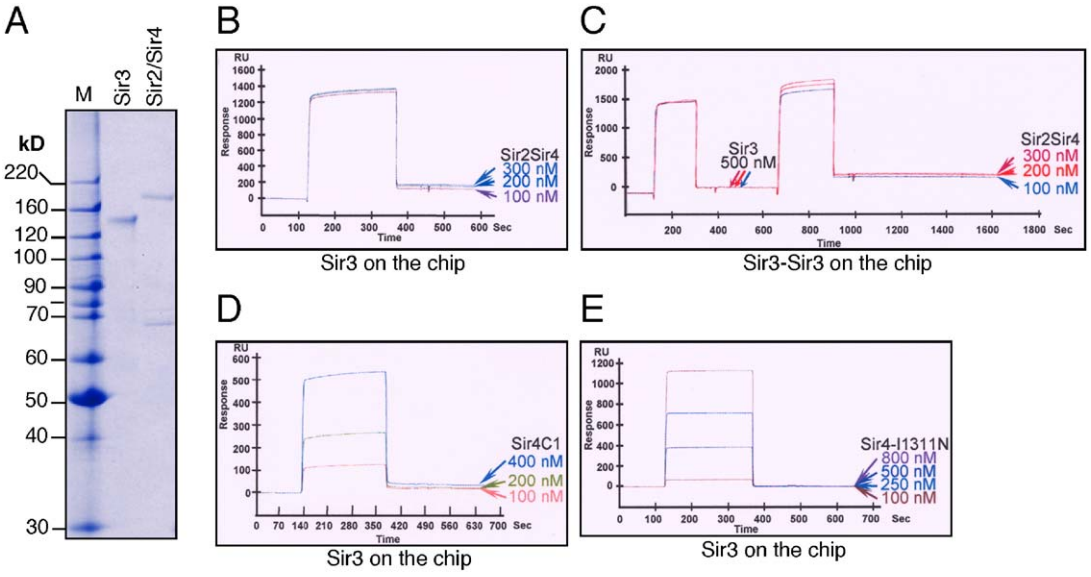

F

Interaction	k_a ($M^{-1}s^{-1}$)	k_d (s^{-1})	K_D (M)
Sir3-Sir2/Sir4	(7.85 +/- 0.74) x 10^4	(2.45 +/- 1.39) x 10^{-6}	(3.26 +/- 2.17) x 10^{-11}
Sir3-Sir3-Sir2/Sir4	(6.83 +/- 0.02) x 10^4	(1.11 +/- 0.65) x 10^{-6}	(1.64 +/- 0.96) x 10^{-11}
Sir3-Sir4C1	(2.06 +/- 0.17) x 10^3	(6.42 +/- 1.14) x 10^{-4}	(3.15 +/- 0.69) x 10^{-8}
Sir3-Sir4C1(I1311)	NM	NM	NM
Sir3-Sir3	(4.36 +/- 1.61) x 10^3	(7.28 +/- 1.60) x 10^{-6}	(1.81 +/- 0.48) x 10^{-9}
Sir3-Sir2	(1.32 +/- 0.32) x 10^4	(7.91 +/- 0.70) x 10^{-4}	(6.30 +/- 1.66) x 10^{-8}

Figure 1. Association of the Sir2/Sir4 Complex with Sir3

(A) Purification of overproduced Sir3-TAP and TAP-Sir4/Sir2 from yeast.

(B–E) Representative surface plasmon resonance experiments showing the binding of Sir2/Sir4 (B) or the C-terminal coiled-coil domain of Sir4 (D) to immobilized Sir3. The spectrum in (C) shows that prebinding of free Sir3 to Sir3 immobilized on the chip results in higher-affinity association of Sir2/Sir4 with Sir3, whereas the spectrum in (E) shows that Sir4-I1311N does not bind to immobilized Sir3.

(F) Summary of *on* (k_a, $M^{-1}s^{-1}$) and *off* (k_d, s^{-1}) rates and the calculated dissociation constants (K_D, M) based on surface plasmon resonance experiments. NM, not measurable. In the interaction column, the protein immobilized on the chip is written in bold lettering.

Sir4 bind to bacterially produced GST fusions containing the amino terminus of histone H4 and (2) a fragment of Sir3 containing amino acids 510 to 970 binds to unacetylated histone H4 peptide with 33 nM affinity (Carmen et al., 2002; Hecht et al., 1995). In these experiments, in contrast to its physiological importance, the acetylation of histone H4-K16 by itself had a modest effect on its interaction with Sir3, whereas a larger decrease in binding was observed upon acetylation of mutiple H4 lysines (Carmen et al., 2002). The availability of highly purified full-length Sir3 and Sir2/Sir4 proteins obtained from yeast provided an opportunity to reexamine SIR-complex interactions with the H4 amino terminus.

We found that Sir3 and the Sir2/Sir4 complex bound to unacetylated histone H4 amino-terminal peptides with 20 and 9 nM dissociation constants, respectively (Figures 2A and 2E). These values are close to what has been previously reported for the interaction of Sir3-Cterm (amino acids 510 to 970) with a similar unacetylated H4 peptide (Carmen et al., 2002). However, in contrast to what has been previously observed for the interaction of the Sir3-Cterm with H4 N-terminal peptides, the association of full-length Sir3 with the H4 N terminus was abolished by acetylation of H4-K16 or all four H4 amino-terminal lysines but was not significantly affected by acetylation of H4-K5 alone or the acetylation of K5, -8, and -12 of H4 (Figure 2E). These results closely mimic the in vivo requirement for the above H4 lysines in silencing where substitutions of H4-K16 severely diminish silencing but substitutions at H4-K5, -K8, and -K12 have little or no effect (Johnson et al., 1990). We conclude that deacetylation of histone H4-K16 is essential for the binding of Sir3 and Sir2/Sir4 to the amino terminus of H4.

Since Sir3 has been proposed to interact with both the H3 and H4 tails as well as additional regions of the nucleosome, we tested the binding of Sir3 to various histone peptides and proteins in SPR experiments in which Sir3 was immobilized on the SPR chip (Figure 2E, lower rows). Sir3 associated with the N terminus of H4 with a K_D of ~90 nM, similar to the value obtained when the peptide was immobilized on the chip, but bound to the N terminus of H3 (amino acids 1 to 20) with lower affinity (K_D of 0.29 μM) (Figure 2E). Recombinant H3/H4 tetramers made with yeast or *Xenopus* histones consistently bound to Sir3 with a 5- to 10-fold higher affinity than a peptide spanning H4 residues

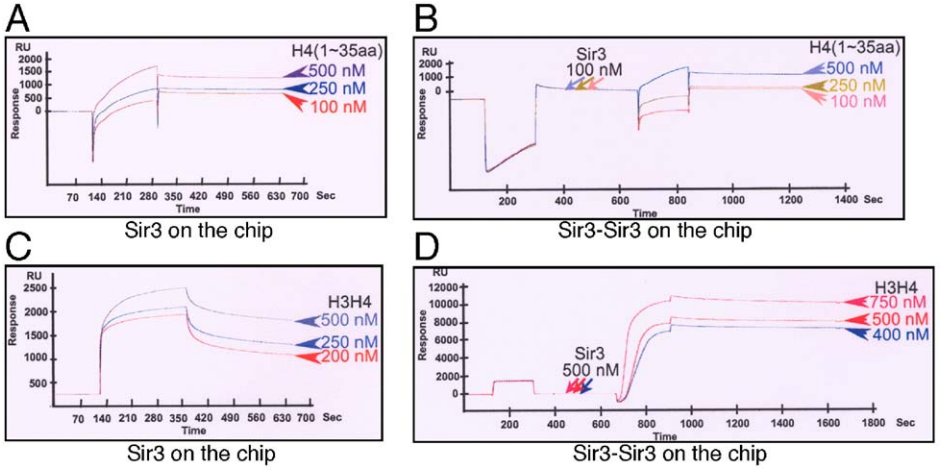

E

Interaction	k_a ($M^{-1}s^{-1}$)	k_d (s^{-1})	K_D (M)
H4-Sir3	(2.25 +/- 0.64) x 10^4	(5.09 +/- 0.51) x 10^{-4}	(2.05 +/- 0.95) x 10^{-8}
H4AcK5-Sir3	(2.39 +/- 0.07) x 10^4	(5.38 +/- 0.79) x 10^{-4}	(2.25 +/- 0.28) x 10^{-8}
H4AcK5/8/12-Sir3	(1.34 +/- 0.11) x 10^4	(6.00 +/- 0.76) x 10^{-4}	(4.51 +/- 0.91) x 10^{-8}
H4AcK16-Sir3	(2.77 +/- 0.58) x 10^3	NM	NM
H4AcK5/8/12/16-Sir3	(1.18 +/- 0.43) x 10^2	NM	NM
H4-Sir2/Sir4	(5.06 +/- 0.86) x 10^4	(4.40 +/- 0.14) x 10^{-4}	(8.91 +/- 1.72) x 10^{-9}
H4AcK5-Sir2/Sir4	(5.54 +/- 0.10) x 10^4	(3.33 +/- 0.18) x 10^{-4}	(6.01 +/- 0.37) x 10^{-9}
H4AcK5/8/12-Sir2/Sir4	(1.31 +/- 0.16) x 10^4	(6.35 +/- 0.73) x 10^{-4}	(4.89 +/- 0.10) x 10^{-8}
H4AcK16-Sir2/Sir4	(2.28 +/- 0.34) x 10^3	NM	NM
H4AcK5/8/12/16-Sir2/Sir4	(2.60 +/- 0.65) x 10^1	NM	NM
Sir3-H4	(5.58 +/- 4.12) x 10^3	(3.33 +/- 2.10) x 10^{-4}	(8.97 +/- 7.15) x 10^{-8}
Sir3-*S.c.*H3/H4	(4.59 +/- 0.68) x 10^4	(4.82 +/- 0.62) x 10^{-4}	(1.07 +/- 0.27) x 10^{-9}
Sir3-*X.l.*H3/H4	(3.30 +/- 1.15) x 10^4	(6.34 +/- 1.34) x 10^{-4}	(2.05 +/- 0.65) x 10^{-8}
Sir3-H3	(1.83 +/- 0.18) x 10^3	(5.06 +/- 3.03) x 10^{-4}	(2.91 +/- 1.94) x 10^{-7}
Sir3-Sir3-H4	(2.28 +/- 1.17) x 10^4	(3.16 +/- 0.53) x 10^{-4}	(1.55 +/- 0.70) x 10^{-8}
Sir3-Sir3-*S.c.*H3/H4	(1.61 +/- 0.42) x 10^5	(2.35 +/- 0.94) x 10^{-5}	(1.42 +/- 0.30) x 10^{-10}
Sir3-Sir3-*X.l.*H3/H4	(2.76 +/- 1.02) x 10^4	(8.93 +/- 0.49) x 10^{-5}	(3.70 +/- 1.39) x 10^{-9}

Figure 2. Acetylation of Histone H4-K16 Abolishes the Association of Sir2/Sir4 and Sir3 with Histone H4 Amino Termini

(A–D) Representative surface plasmon resonance experiments showing the association of histone H4 peptides or histone H3/H4 tetramers with immobilized Sir3. (B) and (D) show that prebinding of additional Sir3 to the Sir3 immobilized on the chip increases the apparent affinity for both the histone peptides and tetramers.

(E) Summary of *on* (k_a, $M^{-1}s^{-1}$) and *off* (k_d, s^{-1}) rates and the calculated dissociation constants (K_D, M) based on surface plasmon resonance experiments. In the interaction column, bold lettering indicates the protein immobilized on the chip. H3 and H4 refer to histone H3 and H4 amino-terminal peptides. H3/H4 refers to bacterially produced histone tetramers.

1–35 (Figures 2C and 2E). This may indicate the presence of additional Sir3 binding surfaces on the tetramer or simply the cooperative contribution of both H3 and H4 tails in the tetramer to binding. In addition, the binding of free Sir3 to Sir3 already immobilized on the chip resulted in a ~5-fold increase in affinity for the H4 amino-terminal peptide as well as H3/H4 tetramers (Figures 2B, 2D, and 2E), suggesting that Sir3 multimerization may increase its affinity for histone tails.

Sir3 Can Self-Assemble into Distinct Oligomeric Forms

The Sir3 protein has previously been shown to interact with itself in two-hybrid assays (Enomoto et al., 2000; Moretti et al., 1994). Because our data suggested that self-association of Sir3 may enhance its affinity for Sir4 and histones (Figures 1 and 2), we used a variety of methods to examine the ability of Sir3 to self-associate. In gel filtration experiments, Sir3 eluted at an apparent size of 600 kDa (Figure 3A), which is consistent with the size of a Sir3 tetramer or, alternatively, an elongated monomer or dimer. However, in native polyacrylamide gels, Sir3 migrated as several species that were consistent with oligomeric states ranging in size from dimers to at least decamers (Figure 3B). The existence of these oligomeric states was confirmed after crosslinking using the bifunctional reagent 1-ethyl-3-(3-dimethylaminopropyl)-carbodiimide hydrochloride/N-hydroxysuc-

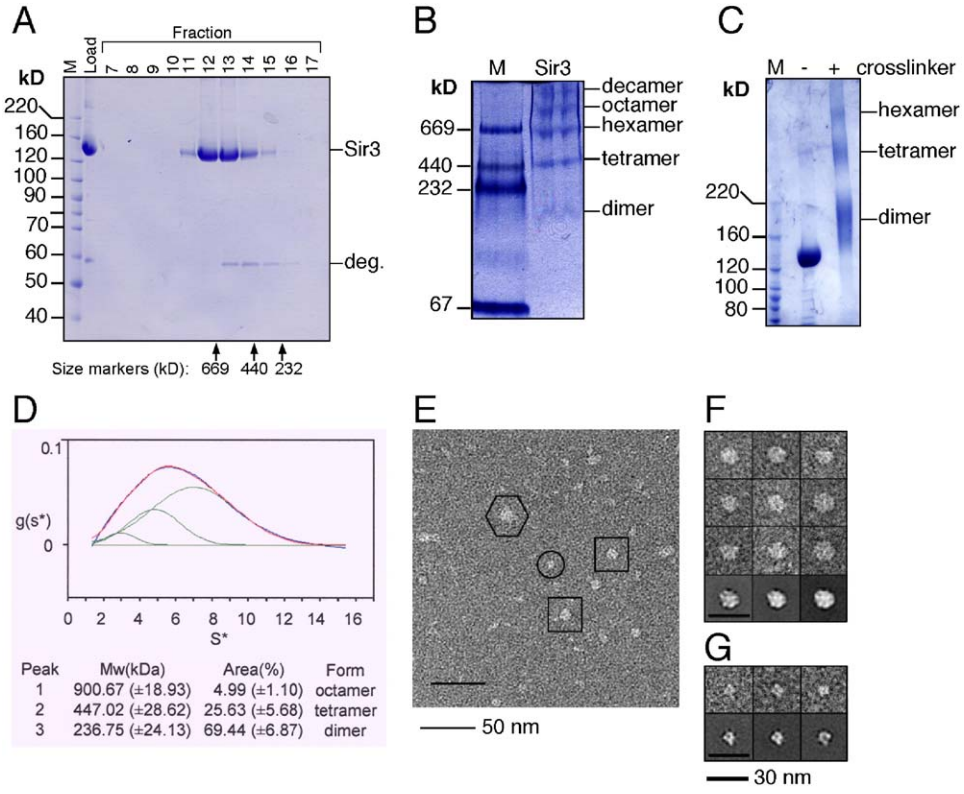

Figure 3. Sir3 Forms Higher-Order Oligomers

(A) Coomassie-stained SDS-polyacrylamide gel showing the migration of Sir3 in a Superose 6 gel filtration column relative to size-calibration markers indicated under the gel (thyroglobulin, 669 kDa; ferritin, 440 kDa; and catalase, 232 kDa). Fraction 12 from the Sir3 peak, which lacks the minor Sir3 degradation product (labeled "deg." in [A]), was used for subsequent experiments in panels (B)–(G).

(B) Coomassie-stained native polyacrylamide gel showing the migration of Sir3 as a mixture of oligomers.

(C) SDS polyacrylamide gel showing the oligomeric states of Sir3 after crosslinking with 1-ethyl-3-(3-dimethylaminopropyl)-carbodiimide hydrochloride/N-hydroxysuccinimide (EDC/NHS).

(D) Analysis of the oligomeric states of Sir3 by velocity sedimentation.

(E) Electron micrograph showing negatively stained Sir3 particles.

(F and G) Selected particles and their respective projection averages (lower rows). Particle sizes in (F) and (G) are consistent with tetrameric and dimeric Sir3 complexes, respectively. Additional image averages are presented in Figure S2.

cinimide (EDC/NHS) and analysis on a denaturing polyacrylamide gel (Figure 3C). Moreover, analysis of Sir3 using equilibrium density centrifugation in an analytical ultracentrifuge revealed a density distribution indicating a mixture of Sir3 dimers to octamers (Figure 3D).

We confirmed the existence of Sir3 oligomers by examining purified Sir3 preparations using negative-stain electron microscopy (EM). As shown in Figure 3E, images of Sir3 preparations revealed particles of heterogeneous size and shape. Classification of these particles using the SPIDER software (Frank et al., 1996) revealed many different classes of particles (Figure S2). The two major classes of particles, large globular particles that are consistent in size with tetramers or octamers and smaller particles that appear to represent dimers, are shown in Figures 3F and 3G, respectively. Projection averages of each class are shown in the lower panels of Figures 3F and 3G, but the round shape and a lack of strong internal features in the particles thwarted our efforts to produce reliable 3D reconstructions. Together, the above results demonstrate that Sir3 can form higher-order oligomers that in solution range in size from dimers to octamers. However, the exact distribution of the various oligomeric forms appears to be sensitive to experimental conditions. For example, tetramers and higher-order oligomers are more prevalent than dimers in native polyacrylamide gels (Figure 3B), whereas in solution dimers are the predominant species (Figures 3C and 3D).

NAD-Dependent Substrate Deacetylation Facilitates the Incorporation of Sir3 into the SIR Complex and Induces a Dramatic Structural Rearrangement

Although SPR spectroscopy experiments showed that the Sir2/Sir4 and Sir3 complexes could interact with a high affinity, a number of previous observations have suggested that the assembly of these proteins into a complex may be a regulated event. For example, only a fraction of Sir3 coimmunoprecipitates with Sir2/Sir4 from yeast extracts (Rudner et al., 2005). To determine whether a SIR complex containing all three Sir proteins could be assembled in solution, we incubated purified TAP-Sir4/HA-Sir2 complexes, immobilized on IgG-Sepharose beads, with purified full-length Sir3 to allow com-

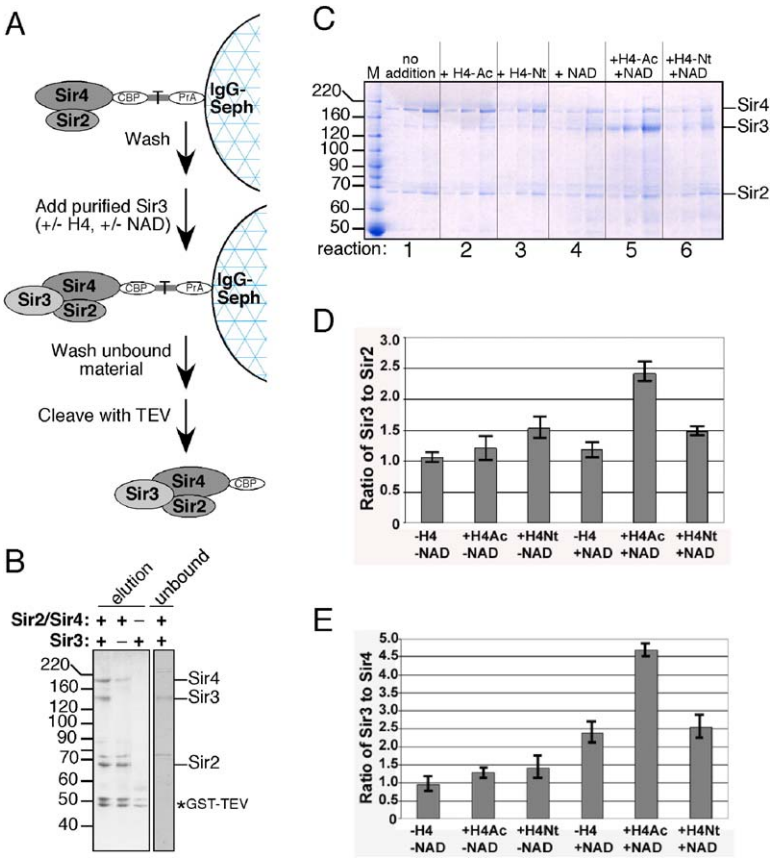

Figure 4. NAD-Dependent Substrate Deacetylation Modulates the Stoichiometry of the SIR Complex

(A) Strategy for assembly of the SIR complex.

(B) Coomassie-stained gel showing the association of stoichiometric amounts of Sir3 with Sir2/Sir4. The position of residual TEV protease used for cleavage is indicated.

(C) Increasing amounts of Sir3 are associated with Sir2/Sir4 in the presence of NAD and a tetra-acetylated histone H4 peptide (H4-Ac). For each assembly reaction (1–6), three 2-fold serial dilutions, right to left, were run on an SDS polyacrylamide gel and stained with Coomassie.

(D and E) Quantification of band intensities from at least three independent experiments are presented and show that, in the presence of NAD and an acetylated histone peptide, the relative ratio of Sir3 to Sir2 and Sir4 increases 2.5- to 4.5-fold, respectively. Error bars represent standard deviation from the mean. H4Nt, unacetylated H4 N-terminal peptide.

plex formation. Following the removal of unbound Sir3 by several washes, the entire complex was eluted using TEV protease as diagrammed in Figure 4A. Gel electrophoresis of the bound and unbound fractions and Coomassie staining showed that this scheme resulted in the assembly of a near stoichiometric 1:1:1 complex containing Sir2, Sir3, and Sir4 (Figure 4B).

We noticed that substoichiometric amounts of Sir3 bound to the Sir2/Sir4 complex at shorter incubation times. These conditions allowed us to test whether histone H4 peptides and/or Sir2 enzymatic activity could enhance the formation of a complete SIR complex. Using shorter incubation times, we performed a series of binding experiments in the presence of histone peptide substrates and NAD and analyzed 2-fold dilutions of eluted SIR complexes by Coomassie staining to allow an estimation of the relative amount of Sir3 bound to Sir2/Sir4. Under these conditions, small amounts of Sir3 bound to the Sir2/Sir4 column in the absence of an H4 peptide (Figure 4C, reaction 1). In the absence of NAD, the addition of an H4 peptide, whether acetylated or not, had no effect on complex assembly (Figure 4C, reactions 2 and 3, respectively). Surprisingly, in the presence of NAD, addition of a tetra-acetylated H4 peptide to the reaction resulted in a marked increase in the amount of Sir3 bound to Sir2/Sir4 (Figure 4C, compare reactions 4 and 5). In contrast, unacetylated H4 did not cause an increase in the amount of Sir3 bound to Sir2/Sir4 even in the presence of NAD (Figure 4C, compare reactions 4 and 6). Quantification of band intensities showed that the presence of NAD and an acetylated histone H4 peptide increased the ratio of Sir3 to Sir2 by approximately 2.5-fold (Figure 4D) and Sir3 to Sir4 by approximately 4.5-fold (Figure 4E) under these assembly conditions. We also observed a small increase in the ratio of Sir3 to Sir4 in reactions that contained NAD, but this increase appears to be due to the loss of some Sir4 from the SIR complex (Figure 4C, compare reactions 1 and 4; Figure 4E). In control experiments using a Sir2/Sir4 complex that contained an enzymatically inactive Sir2-H364Y protein, no increase in assembly was observed under any of the above conditions (data not shown). These results demonstrate that active deacetylation of a histone substrate by Sir2 affects the interaction of Sir3 with Sir2/Sir4 and increases the relative ratio of Sir3 to Sir2 and Sir4 in the complex.

Examination of the above assembly reactions by EM revealed that active substrate deacetylation was accompanied by a dramatic structural rearrangement in SIR particles. Particles from assembly reactions that lacked NAD or contained NAD and an unacetylated histone H4 peptide appeared as globular structures with a diameter of about 20 nm (Figure 5A and Figure S3). Most of the particles from reactions that contained a tetra-acetylated, instead of an unacetylated, histone H4 peptide but were otherwise identical appeared as elongated cylinders of various sizes (Figure 5B). In general, in the absence of NAD-dependent deacetylation, nearly all of the observed particles on the grid appeared globular, whereas upon substrate deacetylation more than 80% of the particles adopted the cylindrical conformation (Table 1; Figure S3). The variation in particle size

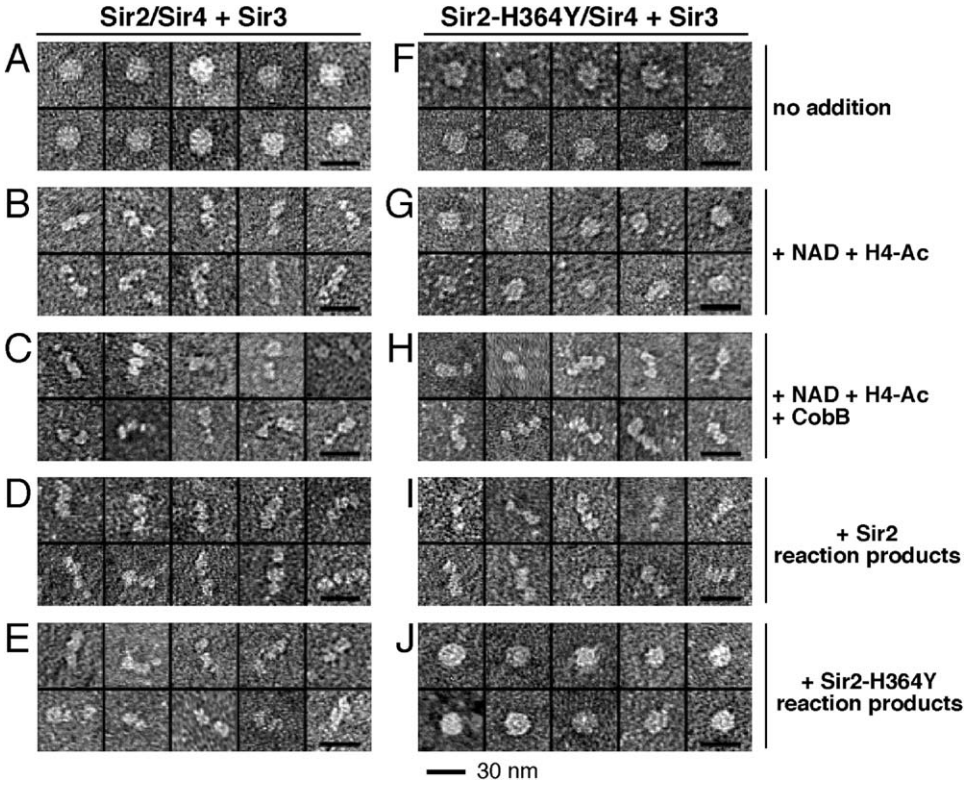

Figure 5. Electron Micrographs Showing that NAD-Dependent Deacetylation Promotes a Structural Rearrangement in SIR Particles

(A–E) SIR particles assembled as described in Figure 4 using enzymatically active Sir2.

(F–J) SIR particles assembled with the enzymatically inactive Sir2-H364Y protein. Reaction conditions are indicated on the right of each panel. Ten representative particles for each assembly condition are shown. A summary of the distribution of different SIR-particle morphologies is presented in Table 1.

may represent the existence of different ratios of Sir3 to Sir2/Sir4 in individual particles.

To further demonstrate that the above structural rearrangement required the enzymatic activity of Sir2, we purified complexes that contained an enzymatically inactive mutant Sir2 protein containing a substitution of the conserved histidine 364 to tyrosine (Sir2-H364Y) (Tanny and Moazed, 2001). This point mutation does not affect the stability of Sir2 or its ability to assemble into a complex with Sir4 (Rudner et al., 2005; Tanny et al., 1999). In contrast to complexes containing wild-type Sir2, particles from assembly reactions containing Sir2-H364Y/Sir4 had a globular appearance in the presence of NAD and the acetylated H4 peptide (compare Figures 5B and 5G), demonstrating that NAD-dependent deacetylation was responsible for the observed structural changes in the SIR particles in our assembly reactions.

We next asked whether the products of NAD-dependent deacetylation could promote the globular-to-cylindrical structural transition in *trans*. The bacterial Sir2-like protein, CobB, deacetylates histone substrates using a reaction mechanism that is identical to Sir2 and produces AAR (Tanner et al., 2000). We added CobB to assembly reactions that contained the enzymatically inactive Sir2-H364Y/Sir4 complex, Sir3, acetylated H4 peptide, and NAD. As shown in Figures 5C and 5H, the addition of CobB could compensate for lack of activity in the Sir2-H364Y/Sir4 complex and promoted the globular-to-cylindrical transition to an extent similar to that observed in reactions containing wild-type Sir2 (Table 1). Furthermore, we performed deacetylation reactions using immobilized Sir2/Sir4 complexes and tested whether the supernatant of reactions containing the products of NAD-dependent deacetylation could promote the structural rearrangement in SIR particles. As shown in Figures 5D and 5I, the products of NAD-dependent deacetylation promoted the globular-to-cylindrical transition in the enzymatically inactive Sir2-H364Y/Sir4/Sir3 particles. On the other hand, the products of a mock deacetylation reaction containing the enzymatically inactive Sir2-H364Y had no effect on the appearance of the Sir2-H364Y/Sir4/Sir3 particles (Figure 5J). Finally, the observed structural changes required the presence of all three Sir proteins, and the addition of nicotinamide, another product of NAD-dependent deacetylation, did not affect the appearance of the SIR particles (Figure 4C, Figure S3, and data not shown). These experiments suggest that the product of NAD-dependent deacetylation, AAR, acts on one of the proteins in the complex to promote the association of Sir3 with Sir2/Sir4 and induce a structural rearrangement in the resulting complex.

To determine whether purified AAR could promote SIR-complex assembly and induce a structural change in SIR particles, we performed large-scale deacetyla-

Table 1. Morphological Classification of SIR Particles Using Electron Microscopy

Reaction Condition	Globular	Nonglobular
Sir2/Sir4 + Sir3 + NAD + H4-Ac	39[a] (17.5%)[b]	184 (82.5%)
Sir2-H364Y/Sir4 + Sir3 + NAD + H4-Ac	>200 (>99%)	—
Sir2/Sir4 + Sir3 + NAD + H4-Ac + CobB	88 (34.9%)	164 (65.1%)
Sir2-H364Y/Sir4 + Sir3 + NAD + H4-Ac + CobB	122 (40.0%)	208 (60.0%)
Sir2/Sir4 + Sir3 + Sir2-H364Y reaction products	48 (21.2%)	178 (78.8%)
Sir2/Sir4 + Sir3 + Sir2-H364Y reaction products	>200 (>99%)	—
Sir2/Sir4 + Sir3 + Sir2 reaction products	86 (14.2%)	520 (85.8%)
Sir2-H364Y/Sir4 + Sir3 + Sir2 reaction products	53 (19.5%)	219 (80.5%)

[a] Particle numbers.
[b] Percentage of total.

tion reactions using the highly active yeast Sir2-like protein Hst2 and purified the resulting reaction products on a C_{18} HPLC column (Figure 6A). Each of the peaks from the C_{18} column was analyzed by matrix-assisted laser desorption/ionization-time of flight (MALDI-TOF) mass spectrometry and identified the expected mixture of acetylated and partially deacetylated histone peptides, unconsumed NAD, and AAR (Figure 6B and data not shown). AAR eluted from the column as two peaks, which are likely to represent 2′-AAR and 3′-AAR. We also employed a simpler thin-layer chromatography (TLC) assay to visualize the products of NAD-dependent deacetylation and their relative purity (Figure 6C). Consistent with the mass spectrometry results (Figure 6B), TLC analysis confirmed that one of the two AAR peaks was pure and lacked detectable NAD (Figure 6C, lane 6). This AAR peak was therefore used in assembly reactions. As shown in Figure 6D, purified AAR increased the ratio of Sir3 to Sir2/Sir4 in SIR-complex assembly reactions (by approximately 2-fold relative to Sir2). Furthermore, in the presence of an unacetylated H4 peptide, AAR promoted the globular-to-cylindrical structural rearrangement in SIR particles (Figure 6E). The above AAR-induced changes in the stoichiometry and appearance of the SIR particles required all three Sir proteins as well as an unacetylated H4 peptide (data not shown). We conclude that AAR, a product of NAD-dependent deacetylation, acts together with a deacetylated histone tail to regulate SIR-complex assembly.

Discussion

Our analysis of the assembly of Sir2, Sir3, and Sir4 into the SIR complex has revealed a role for active NAD-dependent substrate deacetylation in this process. We find that purified Sir proteins can assemble together into a stoichiometric complex. Moreover, Sir2-dependent deacetylation of a histone substrate, which is coupled to NAD hydrolysis and the generation of *O*-acetyl-ADP-ribose (AAR), increases the amount of Sir3 relative to Sir2 and Sir4 in the complex. This change in stoichiometry is accompanied by a dramatic change in the shape of Sir particles visualized by EM. Reconstitution experiments demonstrate that AAR acts together with the deacetylated histone substrate to modulate SIR-complex stoichiometry and structure. Our results also reveal that Sir3 and Sir2/Sir4 bind to histone H3 and H4 amino termini in a manner that is remarkably sensitive to the acetylation state of these regions.

The Association of Sir3 and Sir2/Sir4 with the Amino Terminus of H4 Requires Deacetylation of H4-K16

The amino termini of histones H3 and H4 play a critical role in silencing. Deletion of the H4 tail abolishes silencing at telomeres and plays a redundant role with H3 at the mating-type loci (Kayne et al., 1988; Thompson et al., 1994). Although all four lysines (K5, -8, -12, and -16) in the amino terminus of histone H4 are hypoacetylated in silent chromatin domains, genetic evidence suggests that deacetylation of H4-K16 is particularly important (Johnson et al., 1992; Johnson et al., 1990; Thompson et al., 1994). Whereas substitutions of K5, -8, and -12 with amino acids that mimic acetylated lysine only have modest effects on the efficiency of silencing, similar substitutions at K16 abolish telomeric silencing and severely compromise silencing at the *HML* locus. In previous studies using fragments of Sir3, acetylation of H4-K16 resulted in only a modest decrease in the affinity of H4 amino-terminal peptides for Sir3 (Carmen et al., 2002). It had therefore remained possible that H4-K16 deacetylation indirectly promotes the association of silencing proteins with chromatin—for example, through a change in higher-order nucleosome packing (Dorigo et al., 2004; Luger and Richmond, 1998). Our in vitro binding experiments show that acetylation of H4-K16 abolishes the interaction of full-length Sir3 as well as Sir2/Sir4 with the amino terminus of H4. In contrast, acetylation of H4-K5, -K8, and -K12 has no effect on the interaction of Sir complexes with H4. These results suggest that the critical role of H4-K16 in silencing stems from its direct role in regulating the binding of the SIR complex to chromatin.

A Direct Role for NAD-Dependent Deacetylation in Assembly of the SIR Complex

Sir2 is the founding member of an unusual family of histone and protein deacetylases (Blander and Guarente, 2004; Shore, 2000). In contrast to class I and class II deacetylases, which do not require a cofactor and release an acetyl group as acetate, Sir2-family enzymes (also referred to as sirtuins or class III deacetylases) use NAD as a cofactor in the deacetylation reaction and generate AAR and nicotinamide as reaction products. The role of Sir2 in histone deacetylation and its importance for silencing are supported by studies of catalytically inactive Sir2 mutants (Imai et al., 2000; Tanny and Moazed, 2001). However, the possibility that other outcomes of this unusual reaction may also contribute to

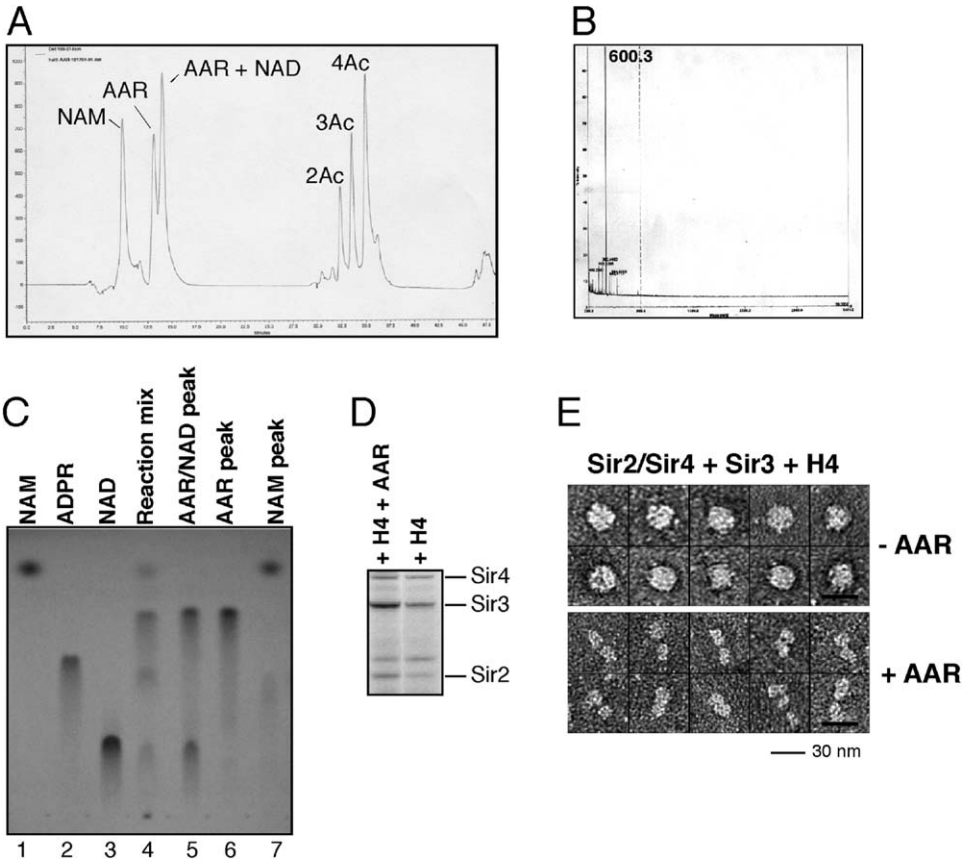

Figure 6. Purified AAR Changes the Stoichiometry and Structure of the SIR Complex

(A) Purification of NAD-dependent deacetylation reaction products on a C_{18} HPLC column. The position of acetylated and deacetylated histone H3 peptides (4Ac, 3Ac, and 2Ac), *O*-acetyl-ADP-ribose (AAR), and NAD as determined by MALDI-TOF mass spectrometry are indicated. The nicotinamide (NAM) peak was identified by thin-layer chromatography (TLC, see [C]).

(B) Mass spectrum showing the molecular mass of AAR from the peak shown in (A).

(C) TLC separation of NAD-dependent deacetylation reaction products (lanes 4–7) and standards (lanes 1–3).

(D) SDS polyacrylamide gel showing that purified AAR promotes the association of Sir3 with Sir2/Sir4.

(E) Electron micrographs showing that purified AAR induces a structural rearrangement in SIR particles. H4, unacetylated H4 N-terminal peptide.

silencing has not been addressed. Our results suggest that the deacetylated histone substrate and AAR act together to modulate the assembly of the SIR complex (Figure 7).

How could AAR modulate SIR-complex assembly? Our results suggest that AAR acts by binding to one of the Sir proteins. In this regard, Sir3 contains an AAA ATPase domain at its C terminus that overlaps with its dimerization and histone binding domains (amino acids 532 to 834) (Neuwald et al., 1999). Structural similarity between AAR and ATP suggests that binding sites for these molecules may also be structurally similar. AAR may bind to this domain in Sir3 and promote a conformation in Sir3 that regulates its interaction with itself and Sir2/Sir4. A second possibility is that Sir2 itself is the target of regulation by AAR. For example, by analogy to ATPases and GTPases, Sir2 may undergo a conformational rearrangement upon NAD hydrolysis that is mediated by binding to AAR. Hst2, a budding-yeast Sir2-like protein, has been crystallized as a ternary complex with AAR and an acetylated peptide, supporting the idea that AAR can remain bound to Sir2-like enzymes after the completion of NAD-dependent deacetylation (Zhao et al., 2003). Since purified AAR has no effect on the structure of Sir3 in the absence of Sir2/Sir4 and vice versa (G.-G.L., unpublished data), regardless of the direct AAR target, all three Sir proteins are required for the observed structural rearrangement.

A central feature of models that describe the spreading of silencing factors along the chromatin fiber is a coupling between the self-association of silencing proteins and their binding to appropriately modified histone tails (Grewal and Moazed, 2003; Grunstein, 1997b; Moazed, 2001; Rusche et al., 2002). In this regard, previous studies have shown that the Sir3 and Sir4 proteins strongly interact with each other and can each form at least dimers (Chang et al., 2003; Moretti et al., 1994). Here we have shown that Sir3 exists as a mixture of dimers and higher-order oligomers. Formation of higher-order oligomers indicates that Sir3 has more than one self-association domain. Although the in vivo significance of this observation remains to be determined, this result raises the possibility that two modes of Sir-protein spreading may be employed: one driven

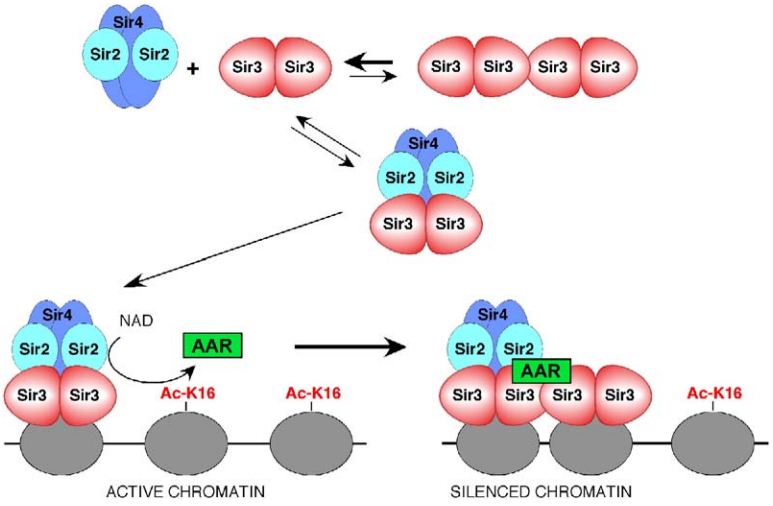

Figure 7. The Role of NAD-Dependent Deacetylation and AAR in Assembly of Silent Chromatin

The SIR complex is assembled from the association of a Sir2/Sir4 complex with dimers of Sir3, which are in equilibrium with higher-order Sir3 oligomers. Recruitment to chromatin and NAD-dependent deacetylation of histone tails by Sir2 promote a structural rearrangement in the complex that is mediated by AAR and association with deacetylated histone tails. H4-K16Ac, whose deacetylation is essential for SIR-complex binding, is highlighted on nucleosomes (gray circles).

by the Sir3-Sir4 interaction and one driven by homotypic interactions between Sir3 dimers (Figure 7).

Implications for the Mechanism of Gene Silencing

Our data strongly suggest that NAD-dependent deacetylation plays a unique role in assembly of silent chromatin. In addition to deacetylation of histone tails, which is critical for binding of the SIR complex to chromatin, the synthesis of AAR modifies the stoichiometry and structure of the SIR complex. We propose that AAR contributes to the formation of a stable chromatin bound SIR complex and provides an additional level of stringency for heterochromatin assembly (Figure 7). The finding that AAR mediates the association of up to three molecules of Sir3 per immobilized Sir2/Sir4 also provides an explanation for previous observations on the unique role of Sir3 in controlling the size of silent chromatin domains. Overexpression of Sir3 results in a dramatic expansion in the size of telomeric silent domains from about 3–5 kb to approximately 20 kb from the chromosome end (Renauld et al., 1993). Remarkably, chromatin immunoprecipitation experiments show that this expansion is associated with the physical spreading of far more Sir3 than Sir2 or Sir4 away from the telomere (Strahl-Bolsinger et al., 1997). Our results suggest that AAR-mediated oligomerization of Sir3 from a nucleation site that contains Sir2/Sir4 may create extended silent chromatin domains that contain more Sir3 than Sir2/Sir4 (Figure 7). Finally, our observations suggest that acetylation of histones in chromatin is required for the assembly of heterochromatin. Although acetyl groups must be removed from specific lysines (e.g., H4-K16) to allow SIR-complex binding, they are also necessary for AAR synthesis and thus actively participate in driving the formation of silent domains. A requirement for acetylated histones, predicted by this model, would provide an explanation for the silencing defects that are observed in cells lacking Sas2 and other histone acetyltransferases (Grienenberger et al., 2002; Meijsing and Ehrenhofer-Murray, 2001).

Sir2-like proteins are conserved in all kingdoms of life and, in addition to gene silencing, play roles in the regulation of metabolism and aging. Our findings raise the possibility that specific targets in these pathways are also regulated by AAR.

Experimental Procedures

Protein Purification and Peptide Synthesis

The strains and plasmids used for overproduction of Sir proteins are described in the Supplemental Data. All histone peptides—H3-Nterm (H3-Nt, amino acids 1–20), H3-K9Ac (same as H3-Nt except acetylated at K9), H3-K4/-K9/-K14/-K18Ac (H3-tetAc), H4-Nt (amino acids 1–35), H4-Nt (amino acids 1–20), H4-K5Ac (amino acids 1–20), H4-K16Ac (amino acids 1–20), H4-K5/-K8/-K12Ac (H4-triAc, amino acids 1–20), and H4-K5/-K8/-K12/-K16Ac (H4-tetAc, amino acids 1–20)—were synthesized by Tufts University Core Facility and HPLC purified.

BIAcore Surface Plasmon Resonance Analysis

Real-time protein-protein interactions were examined using a BIAcore 3000 instrument (BIAcore). Sir3, Sir2His, Sir4C2, Sir3C, H4-Nt, H4-K5Ac, H4-K16Ac, H4-K5/-K8/-K12Ac (H4-triAc), H4-K5/-K8/-K12/-K16Ac (H4-tetAc), and BSA were individually immobilized on different flow cells of a CM5 sensor chip using an amine-coupling kit (BIAcore). Briefly, the chip surface was first activated by injection of 15 μl of 1:1 mixture of 0.4 M N-ethyl-N′-(dimethylaminopropyl) carbodiimide hydrochloride and 0.1 M N-hydroxysuccinimide. Purified Sir3 (10 μl of 100 μg/ml in 20 mM HEPES [pH 8.0], 300 mM KCl, 1 mM $MgCl_2$, and optimal buffer components as determined by trial preconcentration experiments) was immobilized on one flow cell, and an additional flow cell was prepared as a blank background by immobilization of BSA (100 μg/ml) under the same buffer conditions. Remaining activated groups on each flow cell were blocked by injection of 15 μl of 1 M ethanolamine HCl (pH 8.5). The chip was then washed twice with 10 μl of 0.1 M NaOH followed by 10 μl of 0.1% SDS washing to remove any noncovalently bound proteins. Finally, the system was primed with the running buffer A (20 mM HEPES [pH 8.0], 300 mM KCl, 1 mM $MgCl_2$), B (10 mM HEPES [pH 8.0], 100 mM KCl, 1 mM $MgCl_2$), or C (20 mM Tris [pH 8.0], 300 mM KCl, 0.1 mM $MgCl_2$) as indicated. Other proteins or peptide ligands were immobilized using a similar procedure. The interaction assays were performed with a constant (15 μl/min) flow rate at 20°C. Individually distinct concentrations ranging from 50 to 10,000 nM of purified Sir3, Sir2, Sir4C1, Sir2/Sir4, histone H3/H4 tetramers, H3-Nt, H3-K9Ac, H3-tetAc, H4-N1-35 aa, H4-N16-35 aa, H4-Nt, H4-K16Ac, H4-triAc, or H4-tetAc were injected as analytes. The chemical binding groups were regenerated by sequentially washing the analytes with 10 μl injection of 0.1 M NaOH, 0.1 M glycine-HCl (pH 3.5), 10% ethanol, and 0.1% SDS until a back-

ground level was attained. Sensorgrams were subjected to global analysis using BIAevaluation software 3.1. Global fitting analyzed association and dissociation data for ligand-analyte interaction. The simple 1:1 (Langmuir) binding model was employed to fit the data.

Electron Microscopy and Image Processing

2.5 μl of sample was adsorbed to a glow-discharged 200-mesh copper grid covered with carbon-coated collodion film, washed with two drops of distilled water, and stained with two drops of 0.75% uranyl formate. Samples were inspected with an FEI Tecnai T12 electron microscope equipped with a LaB_6 filament and operated at an acceleration voltage of 120 kV. Images were recorded at a magnification of 52,000× and a defocus value of –1.5 μm using low-dose procedures. The micrographs were visually inspected with a JEOL JFO-3000 laser diffractometer, and drift-free images were digitized with a Zeiss SCAI scanner using a step size of 7 μm. Three by three pixels were averaged to yield a pixel size of 4.04 Å at the specimen level. A total of 18,539 Sir3 particles were selected from 74 micrographs using the display program WEB associated with the SPIDER software (Frank et al., 1996), which was used for the subsequent image-processing steps. The selected Sir3 particles were windowed into individual 80 × 80 pixel images and subjected to 10 rounds of multireference alignment and K means classification specifying 50 output classes. The two major subsets of class averages are presented in Figures 3F and 3G. The Sir2/Sir4 particles shown in Figure S2A were imaged using the carbon-sandwich cryonegative staining method (Ohi et al., 2004).

Gel Filtration Chromatography, Gel Electrophoresis, Western Blotting, Protein Quantification, and Chemical Crosslinking

Gel filtration chromatography was performed on an AKTA FPLC system with a Superose 6 column (Amersham Biosciences) as decribed previously (Tanny et al., 2004). Protein samples were separated on either SDS-PAGE or native gels as indicated and were stained by either Coomassie brilliant blue R520 or amido black 10B to visualize protein or blotted for Western detection using chemiluminescence. AlphaEaseFc (Alpha Innotech) and LAS-1000 plus (Fujifilm) were used to quantify the density of protein bands in Coomassie-stained gels. Chemical crosslinking was performed with EDC/NHS (1-ethyl-3-(3-dimethylaminopropyl)-carbodiimide hydrochloride/N-hydroxysuccinimide) crosslinker (Biacore AB). Purified Sir3 (20 mM Tris-HCl [pH 8.0], 300 mM KCl, 0.1 mM $MgCl_2$) was treated with EDC/NHS for 1.5 hr at room temperature and stopped by adding SDS gel-loading buffer and boiling for 2–5 min.

Analytical Ultracentrifugation

Velocity sedimentation experiments were performed using a Beckman Optima XL-I analytical ultracentrifuge. Briefly, 400 μl of purified Sir3 (0.8 mg/ml) and a reference solution (20 mM Tris-HCl [pH 8.0], 300 mM KCl, 0.1 mM $MgCl_2$, or 20 mM HEPES [pH 8.0], 300 mM KCl, 0.1 mM $MgCl_2$) were loaded into a conventional standard double-sector quartz cell and mounted in an An-60 Ti four-hole rotor. Centrifugation was performed at 20°C at a rotor speed of 20,000 rpm. Data were collected in the continuous mode at a single wavelength (280 nm) with a step size of 0.005 cm with three averages. Data were analyzed using either the Optima XL-A/XL-I analysis software version 4.0 (Beckman/Coulter; Microcal) or the DCDT+ software version 1.16 (Philo, 2000).

In Vitro Assembly of SIR-Silencing Complexes

The Sir2/Sir4 complex was immobilized on IgG-Sepharose via the TEV-cleavable TAP tag containing two protein A repeats and a calmodulin binding peptide at the N terminus of Sir4. The IgG-Sepharose-Sir2/Sir4 resin was then incubated with purified Sir3 in the presence or absence of a histone H4 amino-terminal peptide, with or without NAD, for 2 to 4 hr. After washing to remove unbound ligands, complexes were eluted from the resin using cleavage with TEV protease and analyzed by gel electrophoresis and electron microscopy.

Deacetylation Reactions

Approximately 2.5 mg GST-Hst2 or 0.5 mg TAP-Sir4/Sir2 or TAP-Sir4/Sir2-H364Y was immobilized on glutathione-Sepharose 4B (Amersham Biosciences) or on IgG-Sepharose beads (Amersham Biosciences), respectively. The immobilized GST-Hst2, TAP-Sir4/Sir2, or TAP-Sir4/Sir2-H364Y was incubated with 1 mM β-NAD^+ and 1.5 mM tetra-acetylated histone H3 peptide (for Hst2) or tetra-acetylated histone H4 peptide (for Sir2) in 1.75 ml of 50 mM Tris-HCl (pH 7.5), 50 mM KCl (for Hst2) or HEPES-KOH (pH 7.0), 300 mM KCl, 1 mM $Mg(OAc)_2$ (for Sir2) for 2.5 hr at 30°C followed by overnight at 4°C. Protein bound to the IgG-Sepharose beads was then pelleted by centrifugation, and the enzymatic reaction products in the supernatant were either tested directly or purified as described below.

High Performance Liquid Chromatography (HPLC) and Mass Spectrometry

Large-scale deacetylation reaction products were separated as described with modifications (Borra et al., 2002; Jackson and Denu, 2002). Reaction mixtures were purified by HPLC using a Vydac semipreparative small-pore C_{18} column. The purification conditions were as follows: the column was developed using a gradient of 0% to 8% acetonitrile (ACN) in 20 min followed by 8% to 40% ACN containing 0.05% trifluoroacetic acid in 20 min at a flow rate of 10 ml/min. Product peaks were isolated, identified by MALDI-TOF mass spectrometry, checked for purity by analytical HPLC, and lyophilized. MALDI-TOF mass spectrometry was performed on an Applied Biosystems Voyager-DE workstation using dihydroxybenzoic acid (DHB) as a matrix. Samples were desalted using C_{18} Zip-tip desalting pipette tips and were spotted with an equal volume of saturated DHB. MS data were collected in both positive- and negative-ion modes.

Thin-Layer Chromatography

Two microliters of samples was spotted on TLC aluminum sheets (EM Science), which were developed with water/ethanol/ammonium bicarbonate (30%:70%:0.2 M) solvent for ~85 min at room temperature. After drying, the sheet was visualized by UV illumination and photographed.

Supplemental Data

Supplemental Data include Supplemental Experimental Procedures, Supplemental References, and three figures and are available with this article online at http://www.cell.com/cgi/content/full/121/4/515/DC1/.

Acknowledgments

We thank Christopher Walsh for the use of his HPLC and MALDI-TOF instruments; Ju-Fang Chang, Tom Ellenberger, Roy Frye, Brian Hall, and Megumi Onishi for plasmids; Hilal Lashuel for help with analytical ultracentrifugation; Megumi Onishi for histone H3/H4 tetramers; Yifan Cheng for helpful discussions and advice; Lewis Cantley for helpful discussions and encouragement; and Marc Buhler and Andre Verdel for comments on the manuscript. The molecular EM facility at Harvard Medical School was established by a generous donation from the Giovanni Armenise Harvard Center for Structural Biology and is maintained by funds from the NIH (T.W.). This work was supported by grants from the NIH (D.M.). G.-G.L. is a Heidegger Family Scholar in Cancer Research, D.M. and T.W. were Fellows of the Hellman Foundation, and D.M. is a scholar of the Leukemia and Lymphoma Society.

Received: March 13, 2005
Revised: March 25, 2005
Accepted: March 31, 2005
Published: May 19, 2005

References

Aparicio, O.M., Billington, B.L., and Gottschling, D.E. (1991). Modifiers of position effect are shared between telomeric and silent mating-type loci in S. cerevisiae. Cell *66*, 1279–1287.

Blander, G., and Guarente, L. (2004). The Sir2 family of protein deacetylases. Annu. Rev. Biochem. *73*, 417–435.

Borra, M.T., O'Neill, F.J., Jackson, M.D., Marshall, B., Verdin, E., Foltz, K.R., and Denu, J.M. (2002). Conserved enzymatic production and biological effect of O-acetyl-ADP-ribose by silent information regulator 2-like NAD+-dependent deacetylases. J. Biol. Chem. *277*, 12632–12641.

Braunstein, M., Rose, A.B., Holmes, S.G., Allis, C.D., and Broach, J.R. (1993). Transcriptional silencing in yeast is associated with reduced nucleosome acetylation. Genes Dev. *7*, 592–604.

Bryk, M., Banerjee, M., Murphy, M., Knudsen, K.E., Garfinkel, D.J., and Curcio, M.J. (1997). Transcriptional silencing of Ty1 elements in the RDN1 locus of yeast. Genes Dev. *11*, 255–269.

Carmen, A.A., Milne, L., and Grunstein, M. (2002). Acetylation of the yeast histone H4 N terminus regulates its binding to heterochromatin protein SIR3. J. Biol. Chem. *277*, 4778–4781.

Chang, J.F., Hall, B.E., Tanny, J.C., Moazed, D., Filman, D., and Ellenberger, T. (2003). Structure of the coiled-coil dimerization motif of Sir4 and its interaction with Sir3. Structure (Camb). *11*, 637–649.

Dorigo, B., Schalch, T., Kulangara, A., Duda, S., Schroeder, R.R., and Richmond, T.J. (2004). Nucleosome arrays reveal the two-start organization of the chromatin fiber. Science *306*, 1571–1573.

Enomoto, S., Johnston, S.D., and Berman, J. (2000). Identification of a novel allele of SIR3 defective in the maintenance, but not the establishment, of silencing in Saccharomyces cerevisiae. Genetics *155*, 523–538.

Frank, J., Radermacher, M., Penczek, P., Zhu, J., Li, Y., Ladjadj, M., and Leith, A. (1996). SPIDER and WEB: processing and visualization of images in 3D electron microscopy and related fields. J. Struct. Biol. *116*, 190–199.

Gasser, S.M., and Cockell, M.M. (2001). The molecular biology of the SIR proteins. Gene *279*, 1–16.

Ghidelli, S., Donze, D., Dhillon, N., and Kamakaka, R.T. (2001). Sir2p exists in two nucleosome-binding complexes with distinct deacetylase activities. EMBO J. *20*, 4522–4535.

Gottlieb, S., and Esposito, R.E. (1989). A new role for a yeast transcriptional silencer gene, SIR2, in regulation of recombination in ribosomal DNA. Cell *56*, 771–776.

Grewal, S.I., and Moazed, D. (2003). Heterochromatin and epigenetic control of gene expression. Science *301*, 798–802.

Grienenberger, A., Miotto, B., Sagnier, T., Cavalli, G., Schramke, V., Geli, V., Mariol, M.C., Berenger, H., Graba, Y., and Pradel, J. (2002). The MYST domain acetyltransferase Chameau functions in epigenetic mechanisms of transcriptional repression. Curr. Biol. *12*, 762–766.

Grunstein, M. (1997a). Histone acetylation in chromatin structure and transcription. Nature *389*, 349–352.

Grunstein, M. (1997b). Molecular model for telomeric heterochromatin in yeast. Curr. Opin. Cell Biol. *9*, 383–387.

Guarente, L. (2000). Sir2 links chromatin silencing, metabolism, and aging. Genes Dev. *14*, 1021–1026.

Hecht, A., Laroche, T., Strahl-Bolsinger, S., Gasser, S.M., and Grunstein, M. (1995). Histone H3 and H4 N-termini interact with SIR3 and SIR4 proteins: a molecular model for the formation of heterochromatin in yeast. Cell *80*, 583–592.

Hecht, A., Strahl-Bolsinger, S., and Grunstein, M. (1996). Spreading of transcriptional repressor SIR3 from telomeric heterochromatin. Nature *383*, 92–96.

Hoppe, G.J., Tanny, J.C., Rudner, A.D., Gerber, S.A., Danaie, S., Gygi, S.P., and Moazed, D. (2002). Steps in assembly of silent chromatin in yeast: sir3-independent binding of a Sir2/Sir4 complex to silencers and role for sir2-dependent deacetylation. Mol. Cell. Biol. *22*, 4167–4180.

Imai, S., Armstrong, C.M., Kaeberlein, M., and Guarente, L. (2000). Transcriptional silencing and longevity protein Sir2 is an NAD-dependent histone deacetylase. Nature *403*, 795–800.

Jackson, M.D., and Denu, J.M. (2002). Structural identification of 2′- and 3′-O-acetyl-ADP-ribose as novel metabolites derived from the Sir2 family of beta -NAD+-dependent histone/protein deacetylases. J. Biol. Chem. *277*, 18535–18544.

Jenuwein, T., and Allis, C.D. (2001). Translating the histone code. Science *293*, 1074–1080.

Johnson, L.M., Kayne, P.S., Kahn, E.S., and Grunstein, M. (1990). Genetic evidence for an interaction between SIR3 and histone H4 in the repression of the silent mating loci in Saccharomyces cerevisiae. Proc. Natl. Acad. Sci. USA *87*, 6286–6290.

Johnson, L.M., Fisher-Adams, G., and Grunstein, M. (1992). Identification of a non-basic domain in the histone H4 N-terminus required for repression of the yeast silent mating loci. EMBO J. *11*, 2201–2209.

Kayne, P.S., Kim, U.J., Han, M., Mullen, J.R., Yoshizaki, F., and Grunstein, M. (1988). Extremely conserved histone H4 N terminus is dispensable for growth but essential for repressing the silent mating loci in yeast. Cell *55*, 27–39.

Kimura, A., Umehara, T., and Horikoshi, M. (2002). Chromosomal gradient of histone acetylation established by Sas2p and Sir2p functions as a shield against gene silencing. Nat. Genet. *32*, 370–377.

Klar, A.J.S., Fogel, S., and MacLeod, K. (1979). *MAR1*—a regulator of HMa and HMα loci in *Saccharomyces cerevisiae*. Genetics *93*, 37–50.

Landry, J., Sutton, A., Tafrov, S.T., Heller, R.C., Stebbins, J., Pillus, L., and Sternglanz, R. (2000). The silencing protein SIR2 and its homologs are NAD-dependent protein deacetylases. Proc. Natl. Acad. Sci. USA *97*, 5807–5811.

Luger, K., and Richmond, T.J. (1998). The histone tails of the nucleosome. Curr. Opin. Genet. Dev. *8*, 140–146.

Luo, K., Vega-Palas, M.A., and Grunstein, M. (2002). Rap1-Sir4 binding independent of other Sir, yKu, or histone interactions initiates the assembly of telomeric heterochromatin in yeast. Genes Dev. *16*, 1528–1539.

Meijsing, S.H., and Ehrenhofer-Murray, A.E. (2001). The silencing complex SAS-I links histone acetylation to the assembly of repressed chromatin by CAF-I and Asf1 in Saccharomyces cerevisiae. Genes Dev. *15*, 3169–3182.

Moazed, D. (2001). Common themes in mechanisms of gene silencing. Mol. Cell *8*, 489–498.

Moazed, D., and Johnson, D. (1996). A deubiquitinating enzyme interacts with SIR4 and regulates silencing in S. cerevisiae. Cell *86*, 667–677.

Moazed, D., Kistler, A., Axelrod, A., Rine, J., and Johnson, A.D. (1997). Silent information regulator protein complexes in Saccharomyces cerevisiae: a SIR2/SIR4 complex and evidence for a regulatory domain in SIR4 that inhibits its interaction with SIR3. Proc. Natl. Acad. Sci. USA *94*, 2186–2191.

Moretti, P., Freeman, K., Coodly, L., and Shore, D. (1994). Evidence that a complex of SIR proteins interacts with the silencer and telomere-binding protein RAP1. Genes Dev. *8*, 2257–2269.

Neuwald, A.F., Aravind, L., Spouge, J.L., and Koonin, E.V. (1999). AAA+: A class of chaperone-like ATPases associated with the assembly, operation, and disassembly of protein complexes. Genome Res. *9*, 27–43.

Ohi, M., Li, Y., Cheng, Y., and Walz, T. (2004). Negative Staining and Image Classification—Powerful Tools in Modern Electron Microscopy. Biol. Proced. Online *6*, 23–34.

Philo, J.S. (2000). A method for directly fitting the time derivative of sedimentation velocity data and an alternative algorithm for calculating sedimentation coefficient distribution functions. Anal. Biochem. *279*, 151–163.

Renauld, H., Aparicio, O.M., Zierath, P.D., Billington, B.L., Chhablani, S.K., and Gottschling, D.E. (1993). Silent domains are assembled continuously from the telomere and are defined by promoter distance and strength, and by SIR3 dosage. Genes Dev. *7*, 1133–1145.

Rine, J., and Herskowitz, I. (1987). Four genes responsible for a position effect on expression from HML and HMR in Saccharomyces cerevisiae. Genetics *116*, 9–22.

Rudner, A.D., Hall, B.D., Ellenberger, T. and Moazed, D. (2005). A non-histone protein-protein interaction required for assembly of the SIR complex and silencing. Mol. Cell. Biol., in press.

Rusche, L.N., Kirchmaier, A.L., and Rine, J. (2002). Ordered nucleation and spreading of silenced chromatin in Saccharomyces cerevisiae. Mol. Biol. Cell *13*, 2207–2222.

Rusche, L.N., Kirchmaier, A.L., and Rine, J. (2003). The establishment, inheritance, and function of silenced chromatin in Saccharomyces cerevisiae. Annu. Rev. Biochem. *72*, 481–516.

Sauve, A.A., Celic, I., Avalos, J., Deng, H., Boeke, J.D., and Schramm, V.L. (2001). Chemistry of gene silencing: the mechanism of NAD(+)-dependent deacetylation reactions. Biochemistry *40*, 15456–15463.

Shore, D. (2000). The Sir2 protein family: A novel deacetylase for gene silencing and more. Proc. Natl. Acad. Sci. USA *97*, 14030–14032.

Smith, J.S., and Boeke, J.D. (1997). An unusual form of transcriptional silencing in yeast ribosomal DNA. Genes Dev. *11*, 241–254.

Smith, J.S., Brachmann, C.B., Celic, I., Kenna, M.A., Muhammad, S., Starai, V.J., Avalos, J.L., Escalante-Semerena, J.C., Grubmeyer, C., Wolberger, C., and Boeke, J.D. (2000). A phylogenetically conserved NAD+-dependent protein deacetylase activity in the Sir2 protein family. Proc. Natl. Acad. Sci. USA *97*, 6658–6663.

Strahl-Bolsinger, S., Hecht, A., Luo, K., and Grunstein, M. (1997). SIR2 and SIR4 interactions differ in core and extended telomeric heterochromatin in yeast. Genes Dev. *11*, 83–93.

Suka, N., Luo, K., and Grunstein, M. (2002). Sir2p and Sas2p opposingly regulate acetylation of yeast histone H4 lysine16 and spreading of heterochromatin. Nat. Genet. *32*, 378–383.

Tanner, K.G., Landry, J., Sternglanz, R., and Denu, J.M. (2000). Silent information regulator 2 family of NAD- dependent histone/protein deacetylases generates a unique product, 1-O-acetyl-ADP-ribose. Proc. Natl. Acad. Sci. USA *97*, 14178–14182.

Tanny, J.C., and Moazed, D. (2001). Coupling of histone deacetylation to NAD breakdown by the yeast silencing protein Sir2: Evidence for acetyl transfer from substrate to an NAD breakdown product. Proc. Natl. Acad. Sci. USA *98*, 415–420. 10.1073/pnas.031563798

Tanny, J.C., Dowd, G.J., Huang, J., Hilz, H., and Moazed, D. (1999). An enzymatic activity in the yeast Sir2 protein that is essential for gene silencing. Cell *99*, 735–745.

Tanny, J.C., Kirkpatrick, D.S., Gerber, S.A., Gygi, S.P., and Moazed, D. (2004). Budding yeast silencing complexes and regulation of sir2 activity by protein-protein interactions. Mol. Cell. Biol. *24*, 6931–6946.

Thompson, J.S., Ling, X., and Grunstein, M. (1994). Histone H3 amino terminus is required for telomeric and silent mating locus repression in yeast. Nature *369*, 245–247.

Zhao, K., Chai, X., and Marmorstein, R. (2003). Structure of the yeast Hst2 protein deacetylase in ternary complex with 2′-O-acetyl ADP ribose and histone peptide. Structure (Camb). *11*, 1403–1411.